Testing dark energy using pairs of galaxies in redshift space

E. Jennings,[1,2]* C. M. Baugh[1] and S. Pascoli[2]

[1]*Department of Physics, Institute for Computational Cosmology, Durham University, South Road, Durham DH1 3LE*
[2]*Department of Physics, Institute for Particle Physics Phenomenology, Durham University, South Road, Durham DH1 3LE*

ABSTRACT

The distribution of angles subtended between pairs of galaxies and the line of sight, which is uniform in real space, is distorted by their peculiar motions, and has been proposed as a probe of cosmic expansion. We test this idea using *N*-body simulations of structure formation in a cold dark matter universe with a cosmological constant and in two variant cosmologies with different dark energy models. We find that the distortion of the distribution of angles is sensitive to the nature of dark energy. However, for the first time, our simulations also reveal dependences of the normalization of the distribution on both redshift and cosmology that have been neglected in previous work. This introduces systematics that severely limit the usefulness of the original method. Guided by our simulations, we devise a new, improved test of the nature of dark energy. We demonstrate that this test does not require prior knowledge of the background cosmology and that it can even distinguish between models that have the same baryonic acoustic oscillations and dark matter halo mass functions. Our technique could be applied to the completed BOSS galaxy redshift survey to constrain the expansion history of the Universe to better than 2 per cent. The method will also produce different signals for dark energy and modified gravity cosmologies even when they have identical expansion histories, through the different peculiar velocities induced in these cases.

Key words: cosmology: theory – dark energy – large-scale structure of Universe.

1 INTRODUCTION

One of the primary scientific goals of ongoing and future galaxy surveys is to determine what is responsible for the accelerating expansion of the Universe (Schlegel et al. 2007, 2009; Blake et al. 2010; Laureijs et al. 2010; Schlegel et al. 2011). There are two main considerations which affect current tests of dark energy. First, the differences between the observables expected from competitive cosmological models are small. Secondly, given the huge volumes that will be covered by future surveys, it is likely that systematic errors will dominate the interpretation of the measurements. For both these reasons, it is generally accepted that the dark energy challenge should be tackled using multiple cosmological probes (Albrecht et al. 2006; Peacock et al. 2006). Guided by numerical simulations, we assess a recently proposed test, a version of the Alcock–Paczynski test (Alcock & Paczynski 1979), which uses measurements of galaxy pairs to constrain the cosmological model. We expand the available probes of dark energy by setting out an improved version of the test which we show can distinguish models that otherwise cannot be separated by existing methods.

The Alcock–Paczynski test measures the distortion of a spherical object assuming an incorrect cosmological model is used to compute distances. The version of this test considered here models the distortion in a spherically symmetric distribution of galaxy pair angles in redshift space and was first proposed in a form similar to that used in this paper by Phillipps (1994), who considered the distribution of angles between quasar pairs. Recently, Marinoni & Buzzi (2010) introduced an important revision to this test by considering the angle between pairs of galaxies viewed in redshift space. Building on the work of Marinoni & Buzzi, the method outlined in this paper is a refined geometrical test of dark energy. The critical feature of our extension is the use of *N*-body simulations of different dark energy models to test the idea that measuring the anisotropic distribution of galaxy pairs in redshift space is a useful probe of cosmology. This geometrical test of dark energy will complement and extend currently used geometrical probes such as measuring the light curves of Type Ia supernovae (SNe Ia; Riess et al. 1998; Perlmutter et al. 1999; Riess et al. 2011) and applications of the Alcock–Paczynski test to baryonic acoustic oscillations (BAOs; e.g. Blake et al. 2011).

In a Friedmann–Robertson–Walker universe, pairs of galaxies should be distributed with random orientations if the fundamental assumptions of homogeneity and isotropy are correct. This simple test of cosmology is complicated by two effects: first, we do not observe galaxies directly in real space but in redshift space,

*E-mail: elise.jennings@durham.ac.uk

where peculiar velocities, distinct from the Hubble flow, displace the position of a galaxy along the line of sight from its true position. This introduces a preferred direction, with the result that galaxy pairs are no longer randomly distributed. Secondly, in order to convert observed angles and redshifts into comoving distances, an observer needs to assume a cosmological model. An intrinsically spherical object, such as a cluster of galaxies, or a spherically symmetrical distribution, such as the distribution of galaxy pairs we consider in this paper, will appear distorted if measured assuming a cosmology that does not match the true underlying cosmology of the Universe (Alcock & Paczynski 1979).

Based on this idea, Phillipps (1994) proposed a test where the hypothetical sphere proposed by Alcock & Paczynski (1979) is replaced by randomly oriented quasar pairs. In the absence of peculiar motions, a large sample of quasar pairs should have a uniform distribution in the cosine of the angle between each pair, if the correct cosmology is adopted. Marinoni & Buzzi (2010) developed this test by modelling the effect of the redshift-space distortions as a Doppler shift in the positions of the galaxies. They applied this model to galaxy pairs in the Sloan Digital Sky Survey (SDSS) (Abazajian et al. 2009) at low redshift and the DEEP2 galaxy redshift survey (Coil et al. 2004) at $z \sim 1.3$. After selecting galaxy pairs according to a set of constraints discussed in Section 4, Marinoni & Buzzi were left with a sample of 721 pairs in the seventh data release of the SDSS at $z \sim 0$. Mainly due to the small sample size, Marinoni & Buzzi were only able to distinguish a Λ cold dark matter (ΛCDM) cosmology from somewhat extreme alternatives, namely an Einstein–de Sitter universe and an open universe with no dark energy. We note that these models have already been ruled out by other tests. This does not, however, imply that the test cannot be used to yield competitive constraints on dark energy with a larger sample of pairs. Note that the Alcock–Paczynski test measures a distortion parameter which is proportional to the angular diameter distance at the redshift of the object, $D_A(z)$, multiplied by the Hubble rate, $H(z)$. The test we propose in this paper models the distribution of galaxy pairs in real and redshift space assuming a distant observer approximation. This assumption removes any dependence on the angular diameter distance in the distortion parameter. As a result, this technique allows us to measure the Hubble rate directly.

In this paper, using subhalo pairs in large-volume N-body simulations, we test the method of Marinoni & Buzzi and its potential to distinguish between cosmologies. First, we focus on the selection criteria necessary to provide a homogeneous sample of pairs whose distribution in redshift space agrees with the theoretical model of Marinoni & Buzzi. With robust selection criteria, we then apply this test to different simulations to see if these dark energy models can be distinguished from ΛCDM. A critical assumption made in the analysis by Marinoni & Buzzi is that the normalization of a theoretical model of pair distribution does not evolve with redshift. We show, using numerical simulations, that this assumption is incorrect. We also consider the practical difficulties associated with obtaining an accurate measurement of this normalization parameter observationally. We demonstrate that the test, as originally proposed, suffers from large systematics which limit its utility. We present an improved methodology which uses N-body simulations and does not require prior knowledge of the true cosmological model.

Most attention to date has focused on cosmological tests which require measurements on large scales, such as the rate at which cosmic structures grow (Guzzo et al. 2008; Wang 2008), the apparent location of BAOs (Sánchez et al. 2009; Blake et al. 2010) and the projected matter density as measured through weak lensing (Massey et al. 2007). It is important to expand this arsenal of tests. This intro-

duces sensitivity to different systematics, which, alongside results from other probes, will lead ultimately to a more convincing measurement of the properties of dark energy. Also, it is useful to devise new tests which are not reliant on measuring the galaxy distribution on the very largest scales, thereby avoiding the need for an accurate determination of the mean galaxy density (for another example, see Nusser, Branchini & Davis 2011). The test proposed in this paper requires a large volume simply to accumulate a large sample of galaxy pairs; there is no requirement implied on the accuracy of the photometry across a survey used for this purpose.

A novel feature of our analysis is the use of N-body simulations to validate and improve upon the methodology proposed by Marinoni & Buzzi. Recent work has shown that numerical simulations of structure formation have an important role to play in modelling cosmological probes and assessing potential systematic errors. Angulo et al. (2008) demonstrated that the shape of the power spectrum of galaxy clustering is substantially different from the predictions of linear perturbation theory even on very large scales (see also Smith, Scoccimarro & Sheth 2007; Smith, Scoccimarro & Sheth 2008; Seo et al. 2008; Jennings et al. 2010). The simulation results led to revised analyses of BAOs, which attempt either to model the distortions introduced by non-linearities and redshift space, or to reconstruct the linear theory signal (Seo & Eisenstein 2007; Sánchez, Baugh & Angulo 2008; Montesano, Sánchez & Phleps 2010; Montesano, Sanchez & Phleps 2011). Similarly, N-body simulations have demonstrated that the measurement of the growth factor from redshift-space distortions requires careful modelling (Jennings, Baugh & Pascoli 2011a; Okumura & Jing 2011). Jennings et al. (2011b) showed that a naïve application of a linear theory model for the distortion of clustering in redshift space can lead to a catastrophic misinterpretation of the measured growth factor. The study in this paper is in a similar spirit; the availability of N-body simulations to model the pair distribution allows us to devise an improved cosmological probe.

The outline of this paper is as follows. In Section 2, we review the theoretical model of Marinoni & Buzzi (2010) for the anisotropic distribution of pairs and its dependence on cosmology. In Section 3, we discuss the quintessence dark energy models and the N-body simulations used in this paper. In Section 4, we list and test the selection criteria used to select a homogeneous sample of galaxy pairs from the N-body simulations whose distribution agrees with the theoretical predictions. In Section 5, we present our results, comparing the theory with measurements from simulations, for the two dark energy and the ΛCDM cosmologies and demonstrate that a robust test of cosmology can only be achieved by combining observations with numerical simulations. In Sections 6 and 7, we present our summary and conclusions.

2 THEORETICAL BACKGROUND: THE DISTRIBUTION OF GALAXY PAIRS

Following the derivation and discussion in Marinoni & Buzzi (2010) (see also the alternative derivation in Phillipps 1994), let us consider a pair of gravitationally bound galaxies, A and B, at an observed angular separation, θ, as shown in Fig. 1. In a flat universe, the angle that galaxy B subtends at galaxy A, as measured from the observer's line of sight through A, which we refer to as the tilt angle, t, can be written as

$$\sin^2 t = \left[1 + \left(\cot\theta - \frac{\chi_A}{\chi_B \sin\theta} \right)^2 \right]^{-1}, \quad (1)$$
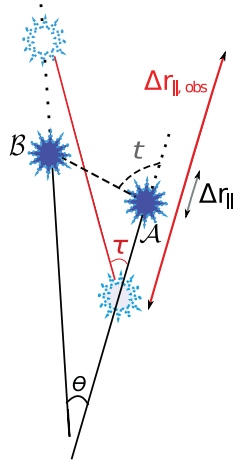
Figure 1. An illustration of the actual, t, and observed, τ, angles subtended between a pair of galaxies, A and B, and the line of sight through A in real space (black) and in redshift space (red). At the observer's position, the pair subtends an angle θ. The comoving line-of-sight separation of the pair is shown as $\Delta r_\parallel$ and $\Delta r_{\parallel,\mathrm{obs}}$ in real and redshift space, respectively.

(see Marinoni & Buzzi 2010 for the general expression in a curved universe). Here $\chi_{A(B)}$ is the radial comoving distance to galaxy $A(B)$ which is given by

$$\chi(z) = \frac{c}{a_0} \int_0^z \frac{\mathrm{d}z'}{H(z')}, \tag{2}$$

where $a = 1/(1 + z)$ is the scalefactor of the universe with current value $a_0 = 1$, c is the speed of light and $H = \dot{a}/a$ is the Hubble parameter with current value $H_0 = 71.5\,\mathrm{km\,s^{-1}\,Mpc^{-1}}$ (Sánchez et al. 2009). In an isotropic and homogeneous universe, the orientation of pairs of bound galaxies will be randomly distributed, allowing us to predict the probability distribution for t, $F(t)$, and a measure of the distribution $\mu = \langle \sin^2 t \rangle$. In the absence of peculiar velocities, an observer calculating the ensemble average of equation (1) should find a value of $\mu = 2/3$, independent of cosmology, as long as the correct cosmology is assumed when converting angles and redshifts to comoving distances for each member of the pair.

Galaxies have velocities in addition to the Hubble flow which result in inferred positions which appear displaced along the line of sight. As a result, the true angle t between a pair of gravitationally bound galaxies will appear as an angle, τ (see Fig. 1). The angle subtended between the pair of galaxies in redshift space, calculated according to equation (1), corresponds to a measurement of the angle τ and not t, and the average over all pairs will no longer be a random distribution. The result is a skewed distribution whose mean will differ from the expected value for a uniform distribution of $\mu = 2/3$. Adopting the correct cosmology to calculate the ensemble average in equation (1) will then provide a measure of the mean of the apparent distribution in redshift space after intrinsic peculiar velocities distort the orientation of the pairs. Marinoni & Buzzi modelled this distortion as a simple Doppler shift where the observed line-of-sight separation is related to the actual separation, to first order in v/c, by

$$\mathrm{d}r_{\mathrm{obs}} = \mathrm{d}r + \frac{\mathrm{d}v_\parallel}{H(z)}(1 + z), \tag{3}$$

where $\mathrm{d}r_{\mathrm{obs}}$ and $\mathrm{d}r$ are the observed and actual line-of-sight separations of a pair of galaxies A and B and $\mathrm{d}v_\parallel = \boldsymbol{v}_A \cdot \hat{\boldsymbol{r}}_A - \boldsymbol{v}_B \cdot \hat{\boldsymbol{r}}_B$ is the line-of-sight peculiar velocity difference, where $\hat{\boldsymbol{r}}_{A(B)}$ represent unit vectors in the direction of each galaxy in the pair. The line-

of-sight comoving separation is $\mathrm{d}r = \mathrm{d}\chi$, as given in equation (2). Note this equation is a result of relating the position observed in redshift space to the actual position in real space as $\mathrm{d}z_{\mathrm{obs}} = \mathrm{d}z + \mathrm{d}v_\parallel$ (see e.g. Hamilton 1998). In the distant observer approximation, the separation between galaxies is assumed to be small compared to the distance between them and the observer. Under this assumption, the observed comoving transverse separation is equal to the true transverse separation of the pair, $\mathrm{d}r_{\perp,\mathrm{obs}} \approx \mathrm{d}r_\perp$. If the redshift difference of the pair Δz is a lot less than unity such that $\Delta z \approx \mathrm{d}z$, then the observed, τ, and actual tilt, t, of the pair can be simply related by the observed, $\Delta r_{\parallel,\mathrm{obs}}$, and the actual line-of-sight finite separation, $\Delta r_\parallel$, according to

$$\frac{\tan t}{\tan \tau} = \frac{\Delta r_{\parallel,\mathrm{obs}}}{\Delta r_\parallel} = 1 + \frac{(1+z)}{H(z)} \frac{\Delta v_\parallel}{\Delta r_\parallel}. \tag{4}$$

The relation given in equation (4) can then be used to transform the true distribution of galaxy pairs, $F(t)$, into the apparent distribution, $\Psi(\tau)$. Using conservation of probability, Marinoni & Buzzi derived the probability distribution function of the apparent angle written in terms of the true angle as

$$\Psi(\tau)\mathrm{d}\tau = F(t)\mathrm{d}t. \tag{5}$$

From this, it follows that $\Psi(\tau)$ is given by

$$\Psi(\tau)\mathrm{d}\tau = \frac{1}{2} \frac{(1+\sigma^2)(1+\tan^2 \tau)}{[1+(1+\sigma^2)\tan^2 \tau]^{3/2}} |\tan \tau| \mathrm{d}\tau, \tag{6}$$

and the parameter σ depends on the cosmological expansion history as

$$\sigma^2(z, \Omega) = 2 \left\langle \frac{\Delta v_\parallel}{\Delta r} \right\rangle \frac{1+z}{H(z)} + \alpha^2 \frac{H_0^2(1+z)^2}{H^2(z)}. \tag{7}$$

The normalization parameter α is given by

$$\alpha = H_0^{-1} \left(\left\langle \frac{\Delta v_\parallel^2}{\Delta r^2} \right\rangle \right)^{1/2}. \tag{8}$$

The first moment of the distribution $\Psi(\tau)$, referred to by Marinoni & Buzzi as the 'average anisotropy of pairs' (the AAP function from now on), is given by

$$\mu_{\mathrm{obs}} = \frac{(1+\sigma^2)\arctan(\sigma) - \sigma}{\sigma^3}. \tag{9}$$

In equation (9), the parameter σ depends on the expansion history in a particular cosmological model, $H(z)$, as given in equation (7). Marinoni & Buzzi set the first term on the right-hand side of equation (7) to zero on the assumption that the comoving separation of pairs and their radial peculiar velocities are uncorrelated, $\langle \Delta v_\parallel / \Delta r \rangle = 0$. We shall discuss this assumption further in Section 4.

The original Alcock–Paczynski test, when applied to a spherical object, measures a distortion parameter, the ratio of the tangential and radial distances, which is proportional to $D_A(z)H(z)$ and is unity if the correct cosmological model is assumed and there are no redshift-space effects, that is, there is no distortion of the spherical object. The Alcock–Paczynski test applied in this paper compares the distribution of pair angles in real and redshift space in the distant observer approximation, $\mathrm{d}r_{\perp,\mathrm{obs}} \approx \mathrm{d}r_\perp$, which gives rise to a distortion parameter which is independent of D_A. The distortion is estimated, after modelling redshift-space effects, by comparing the distribution of the angles t and τ, and only depends on $H(z)$.

Using pairs of galaxies in a survey, an observer can measure the average orientation using equation (1) which should be equal to the AAP function in equation (9) if the correct cosmology is assumed

and the observer is able to measure α precisely in order to fully specify $\Psi(\tau)$. In this paper, we perform this exact test using pairs of subhaloes in N-body simulations of different cosmologies. In practice, in a galaxy survey, the parameter α can be determined in two ways: first, at low redshifts, where the peculiar velocities of the pair can be measured by combining a redshift-independent distance measurement, for example, luminosity distances from SNe Ia, the Tully–Fisher relation or the D_n–σ relation (see e.g. Blakeslee et al. 2000; Borgani et al. 2000; Courteau et al. 2000; da Costa et al. 2000), with the measured redshift of the galaxy. The uncertainties associated with the redshift-independent luminosity distance measurements are large, $\sim$10–20 per cent for the Tully–Fisher or D_n–σ relation, and $\sim$5–10 per cent for SNe or the surface brightness fluctuation method (Bernardi et al. 2001; Tonry et al. 2001). These uncertainties on the redshift-independent distance measurements propagate into larger errors for the peculiar velocities, making it almost impossible to accurately measure the peculiar velocity of a single galaxy. The second method to determine α observationally, which we shall assess in this paper after considering the ideal case of measuring α from the simulations using equation (8), is to fit to the measured distribution of pairs at each redshift using equation (6).

One of the key assumptions made by Marinoni & Buzzi is that the normalization factor α is constant for all redshifts and for different galaxy selections. At $z \approx 0$, Marinoni & Buzzi obtained $\alpha = 5.79^{+0.32}_{-0.35}$, using binaries in the SDSS (Abazajian et al. 2009). Marinoni & Buzzi obtained this value by fitting equation (6) to the observed distribution at $z \approx 0$. We explicitly test this assumption in this paper where it is possible to measure α directly from the N-body simulations at each redshift. We can also compare the predictions of the AAP function using the best-fitting value for α obtained at $z = 0$, instead of normalizing the function at each redshift. This will allow us to see if the value of α really is independent of redshift.

3 TRIAL SAMPLES OF PAIRS FROM NUMERICAL SIMULATIONS

As a test of the method proposed by Marinoni & Buzzi, which was outlined in Section 2, we apply it to different cosmologies, focusing on quintessence models. In Section 3.1, we discuss the two quintessence dark energy models we take as examples and highlight the main differences between these and the concordance cosmological model. In Section 3.2, we describe the simulations carried out.

3.1 Quintessence dark energy

Numerous quintessence dark energy models have been considered as an alternative to the concordance cosmology (see e.g. Ratra & Peebles 1988; Ferreira & Joyce 1998; Copeland, Sami & Tsujikawa 2006; Martin 2008). We focus on two interesting examples which are representative of a wider class of quintessence models, scalar fields which evolve in time, which are viable alternative cosmologies.

One of the models we consider has substantial differences from ΛCDM and can be considered as an 'early' dark energy model which features non-negligible amounts of dark energy at high redshifts. This quintessence dark energy model features an exponential term in the scalar field potential which pushes the dark energy equation of state to $w_0 = -0.82$ today (Brax & Martin 1999). We refer to this model as the SUGRA model. The second quintessence dark

energy model, which we refer to as INV, has been shown to produce a similar expansion history and non-linear growth of structure to those in a ΛCDM cosmology (Jennings et al. 2010, 2011a) and will provide a measure of the sensitivity of the test we perform in this paper. The INV model has an inverse-power-law potential $V(\phi) = \Lambda^{\beta+4}/\phi$ for the scalar field ϕ (Zlatev, Wang & Steinhardt 1999). The values of the constants Λ and β are fixed by the current value of the dark energy density (see e.g. Corasaniti & Copeland 2003).

The dark energy equation of state for these quintessence models can be accurately described over a wide range of redshifts using four parameters (Corasaniti & Copeland 2003). The variables used are: w_0, the current dark energy equation of state; w_m, the value of w during the matter-dominated era; a_m, the scalefactor at which the dark energy equation of state changes from its value during the matter-dominated era to its present value; and Δ_m, the width of the transition in the expansion factor. For the SUGRA model, these parameters are $w_0 = -0.82$, $w_m = -0.18$, $a_m = 0.1$ and $\Delta_m = 0.7$. For the INV model, the values of the parameters are $w_0 = -0.79$, $w_m = -0.67$, $a_m = 0.29$ and $\Delta_m = 0.4$ (Jennings et al. 2010).

The dark energy models have different expansion histories from ΛCDM and so when compared to the currently available observations may favour different best-fitting values of the cosmological parameters (see Jennings et al. 2010, for a discussion). As our starting point, we consider a ΛCDM model with the following cosmological parameters: $\Omega_m = 0.26$, $\Omega_{DE} = 0.74$, $\Omega_b = 0.044$, $h = 0.715$, where $H_0 = 100\,h\,\mathrm{km\,s^{-1}\,Mpc^{-1}}$ and a spectral tilt of $n_s = 0.96$ (Sánchez et al. 2009). The linear theory rms fluctuation in spheres of radius $8\,h^{-1}\,\mathrm{Mpc}$ is set to be $\sigma_8 = 0.8$. In the simulations discussed in this paper, the ΛCDM values for Ω_m and H_0 were used for the INV dark energy model, while for the SUGRA model, the best-fitting parameters used were $\Omega_m = 0.243$ and $H_0 = 67.73\,\mathrm{km\,s^{-1}\,Mpc^{-1}}$ (see Jennings et al. 2010, for more details). Both these models are consistent with current observations of SNe Ia light curves (Kowalski et al. 2008), BAOs (Percival et al. 2007; Sánchez et al. 2009) and the seven-year *WMAP* measurements of the cosmic microwave background (Komatsu et al. 2010). A detailed study of both these models compared to a ΛCDM cosmology can be found in Jennings et al. (2010). Note Jennings et al. (2010) showed that the INV model was indistinguishable from ΛCDM for several cosmological probes such as measurements of the halo mass function, BAO peak positions and growth factor. This model provides us with a significant test of the discriminatory power of the technique proposed in this paper. The ratio of the Hubble parameter in each quintessence dark energy model to that in a ΛCDM cosmology is shown as a function of redshift in Fig. 2.

3.2 N-body simulations

The simulations were carried out at the Institute of Computational Cosmology using a memory efficient version of the TreePM code GADGET-2, called L-GADGET-2 (Springel 2005). The simulations use $N = 646^3 \sim 269 \times 10^6$ particles to represent the dark matter in a computational box of comoving length $1500\,h^{-1}\,\mathrm{Mpc}$. We shall refer to these simulations as the low-resolution runs in Section 5.1. We chose a comoving softening length of $\epsilon = 50\,h^{-1}\,\mathrm{kpc}$. The particle mass in the simulation is $9.02 \times 10^{11}\,h^{-1}\,\mathrm{M_\odot}$ with a mean inter-particle separation of $r \sim 2.3\,h^{-1}\,\mathrm{Mpc}$. We also consider a higher resolution simulation of the ΛCDM cosmology with the same box size as above but with 1024^3 dark matter particles, approximately four times the number of particles used in the lower resolution simulation.
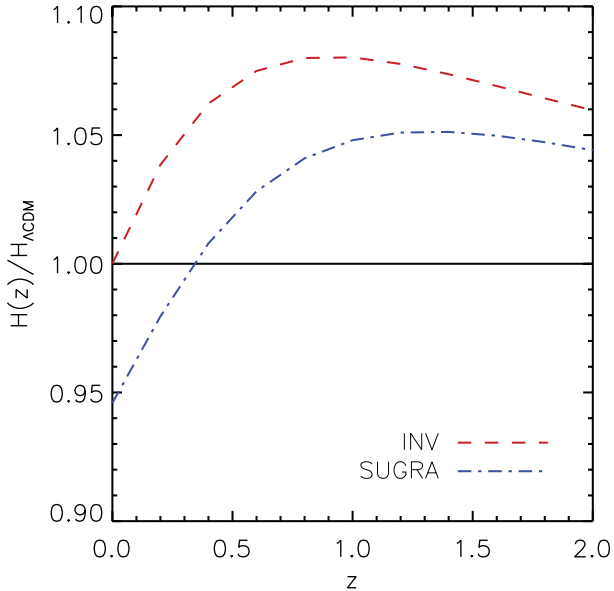
Figure 2. The ratio of the Hubble rate in the two quintessence dark energy models simulated to that in a ΛCDM cosmology plotted as a function of redshift. Note the SUGRA quintessence model has a current value for the Hubble parameter of $H_0 = 67.73 \,\mathrm{km\,s^{-1}\,Mpc^{-1}}$, consistent with observations (see Section 3.1 for details).

The initial conditions of the particle load were set up with a glass configuration of particles (White 1994; Baugh, Gaztanaga & Efstathiou 1995). The particles are perturbed from the glass using the Zel'dovich approximation which can induce small-scale transients in the measured power spectrum. These transients die away after ∼3–10 expansion factors from the starting redshift (Baugh et al. 1995; Smith et al. 2003). In order to limit the effects of the initial displacement scheme, we chose a starting redshift of $z = 200$. The linear theory power spectrum used to generate the initial conditions was created using the CAMB package of Lewis & Bridle (2002). The linear theory power spectrum for the two dark energy models was computed using the parametrized post-Friedmann module (Fang, Hu & Lewis 2008) for CAMB which takes into account the effects of a dynamical dark energy equation of state and dark energy perturbations (Jennings et al. 2010).

Dark matter haloes were identified in the simulation outputs using a Friends-of-Friends (FoF) percolation algorithm with a linking length of $b = 0.2$ times the mean interparticle separation (Davis et al. 1985). The SUBFIND algorithm (Springel et al. 2001) was then run on these halo catalogues to identify self-bound subhaloes at each redshift. Note that the subhaloes are not necessarily bound to the main FoF halo. In this paper, pairs of subhaloes within a common FoF halo are used as a proxy for pairs of galaxies. The minimum number of particles per halo and subhalo is 10 and we select only haloes that have at least two subhaloes (i.e. a minimum of 20 particles in the FoF group). In Fig. 6 (shown later), we show that our results are not affected by our choice of minimum FoF halo mass. The position of each subhalo in redshift space is computed by perturbing its comoving position in real space using the line-of-sight centre-of-mass velocity of the subhalo relative to an observer placed at the origin of the box. At a given redshift $\bar{z} > 0$, the observer is still assumed to be at the origin of the box at $z = 0$ which requires us to add the comoving distance from $z = 0$ to $\bar{z}$ to the subhalo positions. In Section 4, we discuss the selection criteria for subhalo

pairs in relation to the radius R_{200} of the parent halo where the mean density is 200 times the critical value.

4 CALIBRATING THE METHOD USING SIMULATIONS

From the *N*-body simulations we know which pairs of subhaloes are in the same FoF halo. However, this does not guarantee that these objects are gravitationally bound to the FoF halo. There are too many haloes in our simulations to check explicitly for binding, so we will use proxies instead. This will allow us to make contact with the observational selection applied by Marinoni & Buzzi and to see how their cuts translate into cuts in simulation quantities. We investigate these selection criteria and provide robust selection cuts which are independent of cosmology and redshift.

In particular, we address the following question: how do we construct a sample of pairs that match the theoretical expectation for the AAP function, in the most favourable case in which we know the correct cosmology? Using information output from the simulations about the subhaloes selected and the properties of the parent halo (e.g. the FoF algorithm returns R_{200}), we can quantify the definition of a close pair in a rigorous way. If we had selected only bound pairs, we would expect good agreement with the AAP function, provided that we know the correct cosmological model. As a first approach to identify suitable pairs, we shall select subhaloes which are within R_{200} of the main halo, that is, $\Delta r_{\perp,\mathrm{max}} = R_{200}$, with no other restrictions on velocity or distance from a nearest neighbour. As this information is not available to an observer, our second approach will be to translate these selection criteria into observable quantities such as the angle θ between a pair of subhaloes.

Marinoni & Buzzi used the following selection criteria to pick their sample of pairs: (1) a maximum line-of-sight velocity difference of the pair, $\Delta V = 700 \,\mathrm{km\,s^{-1}}$, to avoid projection of neighbouring systems; (2) a maximum comoving transverse separation of $\Delta r_{\perp,\mathrm{max}} = 0.7 \,\mathrm{Mpc}\,h^{-1}$; (3) a minimum comoving transverse separation $\Delta r_{\perp,\mathrm{min}} = 20 \,\mathrm{kpc}\,h^{-1}$; and (4) a minimum comoving distance from the centre of the galaxy pair to another galaxy. The latter two conditions avoid selecting pairs which may be in the process of merging or which are interacting with another galaxy. The value for the maximum velocity difference was chosen such that the relative increase $\Delta N/N$ in the sample size was <1 per cent when the velocity cut was increased by $100 \,\mathrm{km\,s^{-1}}$, while the maximum comoving transverse separation was chosen to be equal to the distance from Andromeda to the Milky Way.

Fig. 3 shows the measured distributions of the orientation of subhalo pairs in real and redshift space in the low-resolution ΛCDM simulation at $z = 0$. The starting point is the sample of subhalo pairs within a common FoF halo, without any further selection. This is shown in real space by the black histogram in Fig. 3. Note that for the lower resolution ΛCDM simulation there are approximately 65 000 subhalo pairs at $z = 0$. The real-space distribution of the tilt follows the expected random distribution and is uniform in $\cos(\tau)$. The distribution of all subhalo pairs in redshift space is shown in red which is clearly skewed. The mean of this distribution differs from the prediction of the AAP function by ∼40 per cent. Applying the final set of cuts to this overall sample as outlined below leaves approximately 19 000 pairs, and produces the blue hashed region which is skewed towards smaller angles and agrees with the predictions of the AAP function given in equation (9) to within 0.5 per cent. We discuss the selection cuts that give rise to this blue
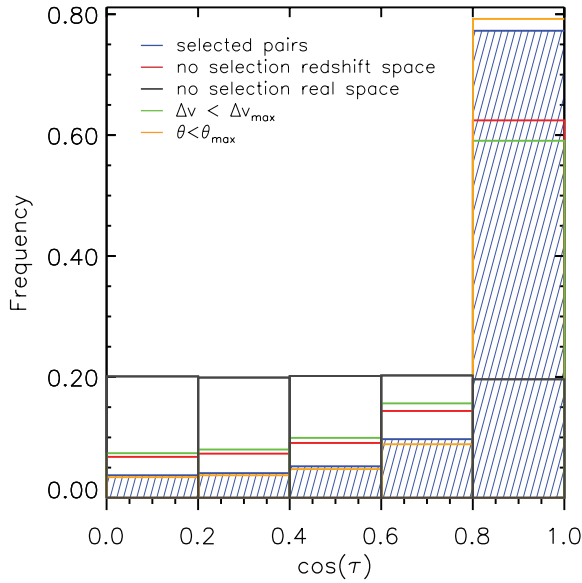
Figure 3. The distribution of the cosine of the apparent inclination angle, $\cos(\tau)$, of pairs of subhaloes in a ΛCDM simulation at $z = 0$. The distribution of $\cos(\tau)$ for all the subhalo pairs in redshift (real) space is shown in red (black). Subhalo pairs that are selected according to the criteria discussed in Section 4 are shown as the blue hashed boxes. Selecting pairs with only a cut in θ_{max} gives rise to the distribution shown in orange. Selecting pairs with only a cut in Δv_{max} gives rise to the distribution shown in green.

hashed region below. A comparison of the red and blue histograms in Fig. 3 shows that in redshift space if no selection cuts are made to isolate bound pairs the distribution is clearly randomized by outliers.
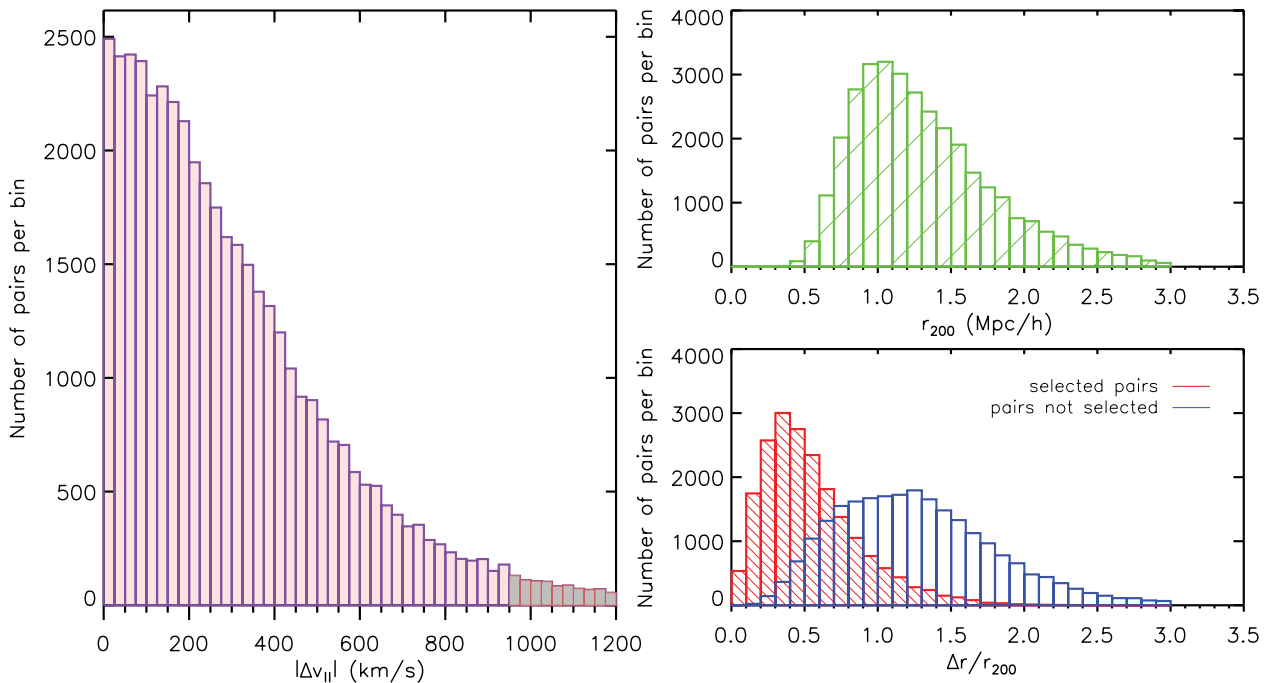
In an attempt to isolate subhaloes that are gravitationally bound to their parent FoF halo and hence to test if their orientations in redshift space are distributed according to the predictions of the AAP function, we first select pairs of subhaloes within R_{200} and exclude all other pairs. We find that this sample of pairs has a non-negligible correlation between $\Delta v_{\parallel}$ and Δr such that $\langle \Delta v_{\parallel}/\Delta r \rangle \neq 0$. As a result, we use the full expression in equation (7) for the parameter σ. This gives an AAP function which is in remarkably good agreement with the measured mean of the distribution, the ensemble average of equation (1), at $z = 0$ in a ΛCDM simulation, to better than a per cent. This agreement diminishes at higher redshifts, with the AAP function and the measured mean differing by 10–20 per cent over the redshift range $z = 0.25$–1.

It is possible to remove subhalo pairs which have $\langle \Delta v_{\parallel}/\Delta r \rangle \neq 0$ by selecting pairs according to an upper limit in the line-of-sight peculiar velocity difference, Δv_{max}. The velocity difference of pairs of galaxies is related to the common gravitational potential of the pair which, in most cases, is weakly correlated with their separation. However, we find that pairs with large velocity differences have non-zero correlations; for example, in the ΛCDM simulation at $z = 0$, using all subhalo pairs with $\Delta v > 950 \, \mathrm{km \, s^{-1}}$ we find $\langle \Delta v_{\parallel}/\Delta r \rangle = 8.5 \, h \, \mathrm{km \, s^{-1} \, Mpc^{-1}}$. Observationally, these subhaloes would not be detected as the apparent tilt between the pair is approximately zero, due to their large peculiar velocity difference, and as a result the pair would lie along the same line of sight. In Fig. 4, we plot the distribution of the line-of-sight peculiar velocity difference Δv in the left-hand panel, for all subhaloes in the lower resolution ΛCDM simulation. The grey shaded region corresponds to the selection cut in Δv. Once we remove any correlated pairs from the sample, and impose the restriction that $\Delta r_{\perp,max} = R_{200}$, we find that the measured mean and the predicted AAP function agree extremely well in the redshift range $z = 0$–2. We present these results in more detail in

Figure 4. Left-hand panel: the distribution of the line-of-sight peculiar velocity difference, $\Delta v_{\parallel}$, for all pairs of subhaloes in the lower resolution ΛCDM simulation at $z = 0$. Pairs to the left-hand side of the grey shaded region represent those subhaloes that have been selected (95 per cent of the distribution). Lower right-hand panel: the comoving transverse separation in redshift space, $\Delta r_{\perp}$, of pairs of subhaloes in the lower resolution ΛCDM simulation at $z = 0$ plotted as a fraction of R_{200}. The selected subhaloes are shown as the red hashed region, while those not selected are shown in blue. Upper right-hand panel: the distribution of the radius, R_{200}, for each parent halo is shown as the green hashed region.

the following section. Note the first term in the expression for σ, equation (7), is now negligible as we have removed any correlated pairs.

As R_{200} is not an observable quantity, the next step is to see if this cut can be translated into a cut in θ, the observed angular separation of the pair. In Fig. 4, we plot the distribution of the comoving transverse separation $\Delta r_\perp$ as a fraction of R_{200} in the lower right-hand panel, for all subhaloes in the lower resolution ΛCDM simulation. The comoving transverse separation $\Delta r_\perp$ as a fraction of R_{200} for the subhaloes that are selected by $\theta < \theta_{max}$ is shown as the red hashed region, while the distribution of those not selected is shown in blue. In the upper right-hand panel in Fig. 4, the distribution of R_{200} for the parent haloes is plotted in green. Selecting pairs according to θ_{max} gives rise to a sample containing most of the subhalo pairs which have $\Delta r_\perp < R_{200}$, with only a small number of pairs with $\Delta r_\perp > R_{200}$ that happen to lie at an angle $\theta < \theta_{max}$.

We find the following selection rules give rise to a population of pairs whose measured moment matches the predictions of the AAP function extremely well, provided the correct cosmological model is assumed (see Section 5.1):

(i) The upper limit of the line-of-sight velocity difference should correspond to retaining 95 per cent of the total distribution of pairs in the sample (grey shaded region in the left-hand panel of Fig. 4).

(ii) The maximum observed separation of a pair, θ_{max}, should correspond to retaining 50–60 per cent of the distribution for all pairs.

Subhalo pairs in redshift space chosen according to the two selection criteria given above give rise to the blue hashed region shown in Fig. 3. For this ΛCDM simulation at $z = 0$, this corresponds to approximately 19 000 pairs with $\Delta v < 950 \, \mathrm{km \, s^{-1}}$ (95 per cent of the distribution) and $\theta < 6.5 \times 10^{-4}$ rad (50 per cent of the distribution). Note these specific values quoted for Δv and θ are only for illustration. The selection criteria presented in the two points above should be applied to the parent sample of galaxy pairs when implementing this test. If we select pairs by restricting Δv only, we retain 38 000 subhalo pairs and then the difference between the measured mean and the corresponding AAP function is approximately 30 per cent. This distribution is shown in green in Fig. 3. Selecting pairs with $\theta < \theta_{max}$ and no restriction on Δv, that is, including correlated pairs with $\langle \Delta v_\parallel / \Delta r \rangle \neq 0$, results in a mean that differs from the corresponding AAP function by less than 1 per cent, provided the full expression for σ in equation (1) is used (shown in orange in Fig. 3). Note if the full expression is not used, then the difference is 4 per cent. We find that the measured moment is most sensitive to the first two selection criteria chosen by Marinoni & Buzzi and relatively insensitive to the minimum comoving separation of the pair and the comoving distance from the nearest neighbour. Note this is partly because we only consider pairs of subhaloes from the same halo.

In Fig. 5, we plot the measured mean of each of the distributions shown in Fig. 3 as a function of redshift. The red dot–dashed line shows the mean of the distribution of all subhalo pairs in redshift space with no cuts. By restricting the sample, using either a cut in Δv or a cut in θ, we obtain the mean shown as the green triple-dot–dashed line and orange dotted line, respectively. Selecting subhalo pairs according to the two selection cuts discussed above results in a measured mean (blue dashed line) which is in very good agreement with the predictions of the corresponding AAP function (solid black line) when we measure α directly from the simulation. Note each distribution has its own associ-
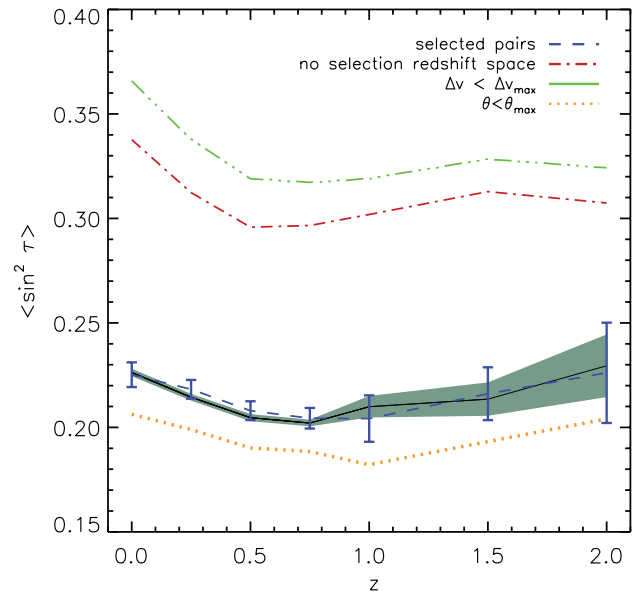

Figure 5. The sample means of the anisotropic distributions of pair tilt angles shown in Fig. 3 for subhaloes in the low-resolution ΛCDM simulation, as a function of redshift. The mean of the distribution of all pairs in redshift space (no selection cuts) is shown as the red dot–dashed line. The measured mean for pairs selected with only a cut in Δv (θ) is shown as the green triple-dot–dashed (orange dotted) line. Once we impose a cut in both Δv and θ, the measured mean of the distribution (blue dashed line) agrees with the corresponding predicted AAP function (solid black line). The light green shaded region shows the uncertainty on this prediction because we have measured α from the simulation which has a finite number of pairs. The AAP function plotted here was found assuming a ΛCDM cosmology for $H(z)$. The error bars on the data points are estimated from a jack knife sampling of the subhalo pairs using 100 subsamples of the data.

ated AAP function, with a normalization set by the pairs in each sample.

The error bars in Fig. 5 have been calculated by jackknife sampling the subhalo pairs by grouping the data into 100 sets containing equal numbers of subhaloes, and then successively removing one set at a time, calculating the sample mean for the remaining haloes and computing the variance amongst the measured means (see Norberg et al. 2009, for a discussion of the reliability of the jackknife technique). We have verified that these errors change the AAP function by less than 1 per cent if we vary the sample size to 25 or 50 subsamples at a given redshift. The error on the AAP function, shown as the green shaded region in Fig. 5, was found using a similar method to find the variance in α at each redshift splitting the pairs in the simulations into 100 subsamples. The errors on both $\langle \sin^2 \tau \rangle$ and the AAP function increase with increasing redshift as the number of pairs decreases. This happens because of the fixed resolution of the simulation, which means that we resolve a progressively smaller fraction of the subhalo population with increasing redshift. A similar drop in the number of pairs would happen in a flux-limited galaxy survey.

We have tested the stability of the method by comparing simulations of different resolution. The sample mean, $\langle \sin^2 \tau \rangle$ (equation 1), of the distribution of subhalo pairs in redshift space in the two ΛCDM simulations, higher and lower resolution, is shown in Fig. 6 at different redshifts. The mean for the lower resolution simulation is shown as the blue squares in Fig. 6. The AAP function using the measured value for α at each redshift is shown as the solid black line as in Fig. 5. The sample mean from the higher
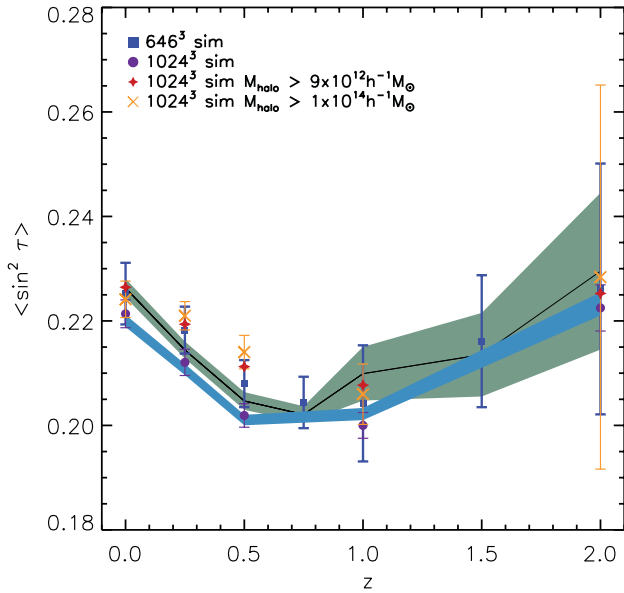
Figure 6. The sample means of the anisotropic distributions of pairs of subhaloes measured in the low- and high-resolution ΛCDM simulations are shown as the blue squares and purple circles, respectively. The AAP function given in equation (9) using the value for α measured from the simulation at each redshift is shown as the light-green and the blue shaded regions for the low- and high-resolution simulations, respectively. The means measured using pairs of subhaloes from the high-resolution simulation that have a parent halo mass of $M \geq 9 \times 10^{12} \, h^{-1} \, M_{\odot}$ and $M \geq 1 \times 10^{14} \, h^{-1} \, M_{\odot}$ are shown as the red stars and orange crosses, respectively. Note that for the measured mean of subhaloes within a parent halo of $M \geq 1 \times 10^{14} \, h^{-1} \, M_{\odot}$ at $z = 2$, there are only 49 pairs and we used 10 subsamples to find the jackknife errors.

resolution simulation is shown as the purple circles with the corresponding AAP function shown as the solid light blue line. In both the lower and higher resolution simulations, the measured distribution of pairs shows excellent agreement with the predictions of the AAP function assuming a ΛCDM cosmology, and also agrees with each other in shape and amplitude within the error bars. The difference between the AAP functions for the higher resolution simulation (blue shading) and for the lower resolution simulation (solid black line) in Fig. 6 is also due to the difference in resolution between the two simulations. If we select only subhaloes from the higher resolution simulation that have a halo mass of $M \geq 9 \times 10^{12} \, h^{-1} \, M_{\odot}$, which corresponds to the minimum halo mass selected by the FoF algorithm in the lower resolution simulation, we obtain the red stars with errors bars plotted in Fig. 6. These points are almost coincident with the corresponding measurement from the lower resolution simulation (blue squares), agreeing to better than 1σ.

We also make contact with an observational galaxy sample in Fig. 6. If we select subhaloes from main haloes which have a mass of $M \geq 1 \times 10^{14} \, h^{-1} \, M_{\odot}$, then we obtain the mean plotted as the orange crosses in Fig. 6. Again these results are consistent with the means for the lower resolution simulation at each redshift. This mass corresponds to the minimum halo mass expected to contain two or more luminous red galaxies (LRGs) on average (Almeida et al. 2008). This subhalo selection is relevant for a spectroscopic redshift survey such as the SDSS-III BOSS (Schlegel et al. 2007) which will target LRGs in the redshift range $z < 0.7$. Without applying any selection cuts, we find approximately 27 000 subhalo

pairs at $z = 0$ which share a common halo of $M \geq 1 \times 10^{14} \, h^{-1} \, M_{\odot}$; at $z = 0.25$ and 0.5, the number of subhalo pairs is approximately 18 000 and 11 000, respectively. From the first semester of BOSS data, White et al. (2011) estimate that the cumulative probability that a galaxy in their sample is hosted by a halo of mass $M \geq 1 \times 10^{14} \, h^{-1} \, M_{\odot}$ is about 5 per cent. If we extend this probability to the full sample of LRGs expected by the BOSS with space density $\bar{n} = 3 \times 10^{-4} \, h^3 \, \mathrm{Mpc}^{-3}$, then this corresponds to approximately 13 000 pairs of LRGs in the redshift range $z = 0.5$–0.6. This is similar to the number of pairs we obtain from the higher resolution simulation restricting to haloes with $M \geq 1 \times 10^{14} \, h^{-1} \, M_{\odot}$ at $z = 0.5$, shown by the orange crosses in Fig. 6.

The errors on the AAP function as measured by Marinoni & Buzzi, $\alpha = 5.79^{+0.32}_{-0.35}$, are substantially larger than ours due to the uncertainty in fitting for the parameter α at $z = 0$ with a smaller number of pairs. Our higher resolution simulation has approximately four times more subhalo pairs than the lower resolution simulation, after making the selection cuts discussed in Section 4, which gives rise to error bars which are approximately 50 per cent smaller in the higher resolution run (see Fig. 6). The sample of pairs used by Marinoni & Buzzi is approximately 25 times smaller than the sample from our lower resolution simulation. We have verified that by applying the Marinoni & Buzzi selection cuts to our parent sample of subhalo pairs in the lower resolution simulation gives $\alpha = 5.69$, which is consistent with the value for α obtained by these authors. However, we find that the measured mean for this simulation sample does not agree with the AAP function within the error bars. (If our sample were of the same size as that used by Marinoni & Buzzi, our errors would be significantly larger and the two would agree in this case.) This demonstrates the need for the robust resolution-independent selection criteria we have presented here.

5 APPLICATION: A NEW TEST

In this section, we use the selection criteria outlined in Section 4 to test the predictions of the AAP function, equation (9), using the distribution of subhalo pair angles measured in *N*-body simulations. The accuracy of this test relies on two key variables: the cosmological expansion history assumed, $H(z)$, and the normalization parameter, $\alpha = H_0^{-1}(\langle \Delta v_{\parallel}^2 \rangle / \langle \Delta r^2 \rangle)^{1/2}$. We consider the impact of uncertainties in each of these variables in turn. In Section 5.1, we present the measured anisotropic distribution of the orientation of pairs, selected according to the prescription set out in Section 4, and its first moment at different redshifts together with the predicted distribution using the AAP function in a ΛCDM cosmology and in two quintessence dark energy cosmologies. In order to test the ability of the theoretical model to distinguish different cosmologies, we will assume perfect knowledge of the correct $H(z)$ and α in the first instance. We then consider how an observer would measure α and the impact this has on the results, again assuming the correct $H(z)$. We relax the assumptions further in Section 5.2 where an incorrect cosmological expansion history is used to analyse the data. This is done by measuring the distribution of subhaloes in the INV and SUGRA dark energy simulations assuming a ΛCDM cosmology to infer distances from the pair. We will show that the method, as implemented in Marinoni & Buzzi (2010), fails to exclude the wrong cosmology. Consequently, we propose a new method, which uses the theoretical model discussed so far but which exploits additional information about α from the numerical simulations. In Section 5.3, we show that this method can be successfully applied to test dark energy.

5.1 Testing the method: theory versus observations

First of all, we test how the approach discussed in Section 2 can distinguish different cosmologies. We put ourselves in the idealized situation of an observer who knows the correct cosmological model to compute distances and is able to measure peculiar velocities precisely to find α at each redshift. In Fig. 7, the mean of the redshift-space distributions of subhalo pairs for ΛCDM and the two quintessence dark energy models are plotted as a function of redshift. The results for ΛCDM are the same as those shown in Fig. 6 for the lower resolution simulation. The measured sample mean for the INV dark energy model is shown as the red-orange circles with error bars, while the results for the SUGRA model are shown as the green-grey triangles. The predicted AAP function for each of these models, using the correct expansion history and the value for α measured at each redshift, is shown as the solid red line for the INV model and as the solid green line for the SUGRA model. The uncertainties on the AAP function are plotted as the red shaded region for the INV model. The errors for the SUGRA model are similar but are not plotted in Fig. 7 for clarity. The errors shown on both models for the measured mean and the AAP function were found using an identical jackknife sampling method to that used for the ΛCDM result. It is clear from Fig. 7 that the measured mean for the three simulations agrees with the respective AAP function, provided the correct expansion history is known and that the parameter α can be determined at each z. As these results show, the measurements in a ΛCDM or a dynamical dark energy model agree very well with the predictions, if the correct cosmology is used to analyse the data. For the two quintessence models, the deviations from ΛCDM are due to the different expansion histories
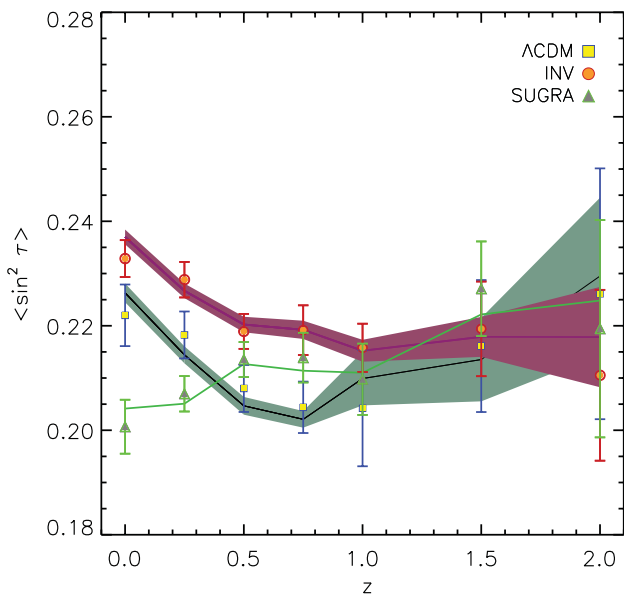
(see Fig. 2). This is a consistency check which confirms that the method works.

In reality, in a galaxy survey, it is not possible to measure the parameter α accurately at high redshifts because of the difficulties associated with measuring galaxy peculiar velocities to sufficient precision. We shall now degrade the status of the idealized observer mentioned above and consider a more realistic observer who still knows the correct cosmological model but who is unable to measure α directly at any redshift other than $z = 0$. Using the measured distribution of pairs at $z = 0$, we fit the distribution given in equation (6) to set α and test the accuracy of the AAP function using this $\alpha(z = 0)$ value at each redshift, as suggested by Marinoni & Buzzi. If α does not evolve with redshift, we would expect this approach to result in accurate agreement between the measured mean and the AAP function.

In Fig. 8, the measured distribution of the angle τ, in radians, for ΛCDM is shown as the red hashed region with error bars. Note the y-axis shows the fraction of the total number of pairs per bin. The distribution (equation 6) with the best-fitting value $\alpha_{FIT} = 5.67 \pm 0.1$ (with 1σ errors) is plotted as the purple dashed line. The grey dotted lines show the distribution adopting $\alpha + 1\sigma$ and $\alpha - 1\sigma$. Note the error we obtain for α, 0.1, is much smaller than that obtained by Marinoni & Buzzi (0.3) due to the difference in sample size and the different methods used to estimate the errors. This value for α agrees with the measured value from the simulations of $\alpha = 5.56$. In Fig. 9, the AAP function assuming a ΛCDM cosmology and using this $\alpha_{FIT}(z = 0)$ value at each redshift is shown as the black dashed line with error bars. The mismatch between this curve and the simulation results clearly indicates that α evolves with redshift, invalidating one of the main assumptions made in the analysis of Marinoni & Buzzi. Note that the black dashed line in Fig. 9 is much smoother than the shaded green band for the AAP function
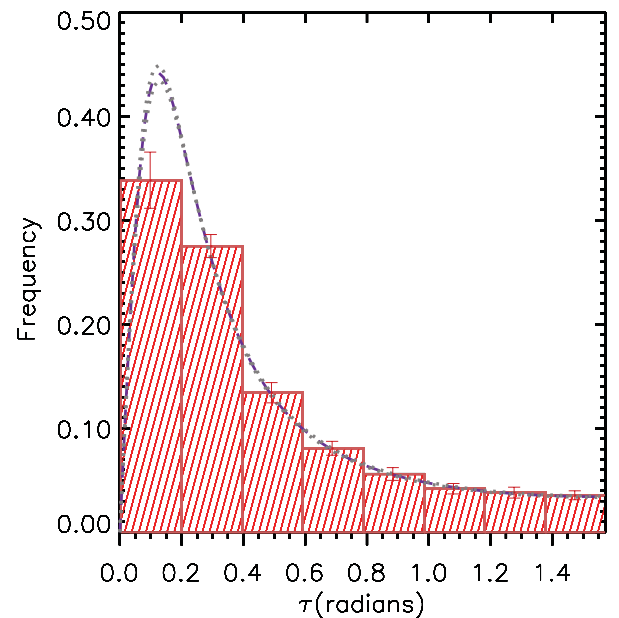

Figure 7. The first moment of the anisotropic distribution of pairs of subhaloes measured in a ΛCDM cosmology and two quintessence dark energy simulations as a function of redshift. Measurements for the ΛCDM, INV and SUGRA cosmologies are shown as the blue squares, red circles and green triangles, respectively. The AAP function using the measured value for α at each redshift for each cosmological model is shown as the solid black, red and green lines for ΛCDM, SUGRA and INV, respectively. The shaded bands show the uncertainty on the AAP function for each cosmology. Note that the error bars for the AAP function for SUGRA are similar to those for the INV model and are not shown for clarity.

Figure 8. The fractional distribution of the angle τ in radians of pairs of subhaloes measured in ΛCDM at $z = 0$. The error bars on each bin are calculated by jackknife sampling after dividing the catalogue of subhalo pairs into 100 subsamples and calculating the variance amongst the distributions measured after successively removing one subsample at a time. The purple dashed line shows the distribution in equation (6), with the best-fitting value of the normalization parameter $\alpha_{FIT} = 5.67 \pm 0.1$. The grey dotted lines show the 1σ error on the best-fitting distribution.
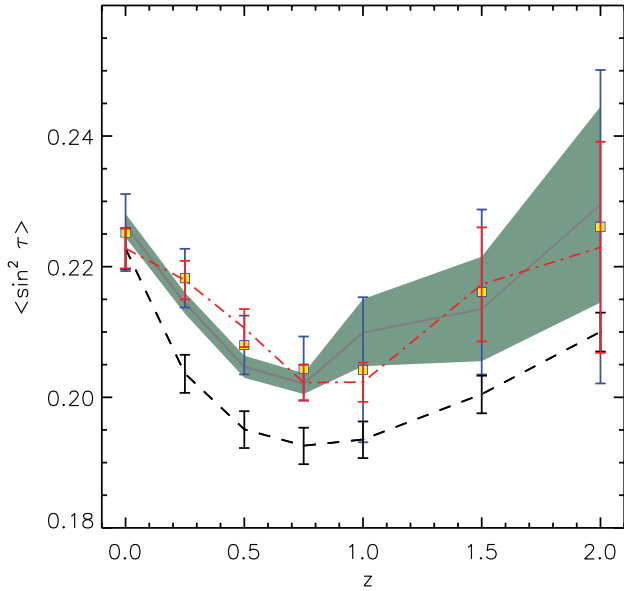
Figure 9. The first moment of the anisotropic distribution of pairs of subhaloes measured in a ΛCDM simulation (blue-yellow squares) as shown in Fig. 7. The AAP function using the $z = 0$ best-fitting value for α at each redshift (see Fig. 8) is shown as the dashed black line with error bars. If we fit for α using the measured distribution at each redshift, then we obtain the red dashed line prediction for the AAP function assuming a ΛCDM cosmology. The error bars on the black dashed and red dot–dashed lines are the 1σ errors obtained by fitting for α.

in ΛCDM where the value of α is measured directly from the simulation at each redshift. Using the $z = 0$ value for α produces an AAP function which is systematically and significantly below the measured results for a ΛCDM cosmology for $z > 0$. Applying this measure of α as proposed by Marinoni & Buzzi could lead to a spurious detection of deviations from ΛCDM. It is clear from Fig. 9 that the method proposed by Marinoni & Buzzi contains a serious systematic error which is apparent when applied to a large sample of pairs. Marinoni & Buzzi considered a smaller sample than in the simulations where the statistical errors dominated this systematic.

It is clear from Fig. 9 that α does evolve with redshift and that we can improve on the estimates of this parameter by fitting equation (6) to the measured distribution at each redshift. In Fig. 9, the AAP function in a ΛCDM cosmology using the best-fitting values for α measured at each redshift is shown as the red dot–dashed line with error bars. The jackknife errors on α are estimated using 100 subsamples for the distributions at $z = 0$–1 and using 50 subsamples for $z = 1.5$ and 2 as there are fewer pairs at these higher redshifts. This approach to measuring α gives much better agreement with the mean measured from the simulations, shown as the blue-yellow data points in Fig. 9. Note this method of extracting α assumes that the correct cosmology is ΛCDM.

5.2 The test assuming a particular cosmology

In this section, we are no longer idealized observers who know the correct cosmology, so the only possible choice is to assume the same cosmology in the data fitting and in the theoretical prediction of the galaxy distribution. Specifically, we will assume ΛCDM, for simplicity, in order to set the expansion history $H(z)$ in equation (8) and to compute the comoving distances in equation (1), as well as to extract the parameter α. In order to find the parameter α, we must

fit to the observed distribution of the orientations of pairs which has been found also by assuming a ΛCDM cosmology. Assuming that the true cosmological model chosen by nature is a dynamical dark energy model, for instance, the INV or SUGRA cosmology, we will check if the wrong cosmology, ΛCDM in our case, can be excluded or not, and consequently if the method is applicable to future galaxy surveys. For this analysis, we take subhalo pairs in the INV and SUGRA simulations, and at each redshift we rescale the comoving distances to match those which would be computed by an observer assuming a ΛCDM cosmology.

The ensemble average of equation (1) for each subhalo pair in the INV (SUGRA) simulation is plotted in Fig. 10 as the red circles (green triangles), with error bars. If we fit for α at each redshift, we obtain the purple dot–dashed line in Fig. 10 for the INV model. Although we have assumed, incorrectly, a ΛCDM cosmology, we find that the AAP function agrees with the measured sample mean for the INV model at each redshift. In Fig. 10, a similar analysis is presented for the SUGRA model. The measured mean for this dark energy model, assuming a ΛCDM cosmology to compute comoving distances, is shown as the green triangles. The AAP function using the best-fitting value for α at each redshift and a ΛCDM expansion history is shown as the grey dashed line. Again, theory and observations agree when we would expect them not to as we have used the wrong cosmology in the AAP function and to compute distances. Our results show that the AAP function, using either a fixed value of $\alpha(z = 0)$ or a best-fitting value at each redshift, is not an accurate model with which to test for dynamical dark energy models if the correct cosmological model is unknown and that further input from numerical simulations is needed to arrive at a viable test.
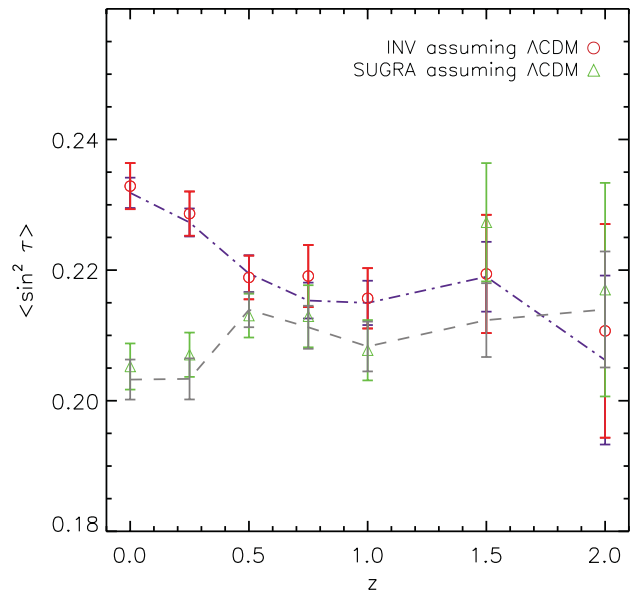

Figure 10. The measured mean of the anisotropic distribution of pairs of subhaloes in the INV dark energy simulation *assuming* a ΛCDM cosmology to find the comoving distance from each pair member (red circles). The purple dot–dashed line shows the predicted AAP function, assuming a ΛCDM cosmology, and using the best-fitting α found at each redshift. The measured mean for the SUGRA model, *assuming* a ΛCDM cosmology, is shown as the green triangles and the predicted AAP function, assuming a ΛCDM cosmology, and using the best-fitting α found at each redshift, is shown as the grey dashed line.

5.3 A blueprint for probing dark energy

From the previous section it is clear that the cosmological test proposed by Marinoni & Buzzi relies heavily on measuring the parameter α accurately at each redshift. The assumption that α does not vary with redshift is incorrect and could falsely rule out ΛCDM if this test is misapplied to pairs of galaxies in future surveys. The value of α also depends on the cosmological model. For example, at $z = 0$, the values for the ΛCDM, SUGRA and INV cosmologies are $\alpha = 5.56$, 6.32 and 5.32 respectively, with a typical error of 0.1. The difficulty is not just a problem of measuring α accurately but stems from the fact that the cosmology assumed affects both the data and the theoretical prediction in a way which cannot be disentangled. The accuracy and predictive power of the AAP function can be restored if instead of measuring α from observations, we employ N-body simulations which contain a comparable number of subhalo pairs to the number of galaxy pairs in the survey under consideration. It is clear that independent information about α is necessary and numerical simulations play an important role in providing these predictions in a given cosmology. We propose a new approach to measuring dark energy, where observational measurements of the mean of the anisotropic distribution of pairs and predictions of the AAP function from numerical simulations are combined. The new method we propose to test a given cosmology is as follows:

(i) An observer assumes the cosmology to obtain the comoving distances needed to calculate the ensemble average of equation (1) for a sample of pairs of galaxies, selected using the criteria given in Section 4, at different redshifts.

(ii) Using an N-body simulation of the same assumed cosmology and with a comparable number density of pairs and volume to the galaxy survey, the observer can then construct a similar catalogue of pairs according to Section 4 and find the value of α at each redshift.

(iii) This gives rise to a prediction for the AAP function which can be compared with the means measured from the galaxy survey at each redshift, and the assumed cosmology can be verified or excluded.

Note if the AAP function measured from the simulation and the measured mean of the galaxy pair sample analysed assuming the same cosmology disagree, then a suite of N-body simulations of different cosmologies would need to be run. The AAP function from each simulation should then be compared to the measured mean, computed assuming the cosmology used in the simulation. This test is realistic, given current computing resources. In Fig. 11, we use the INV and SUGRA simulations to illustrate this method. In the upper and lower panels, we show the measured means for the INV and SUGRA dark energy simulations, respectively, which are treated here as the 'observed' pair sample. In this example, we are testing a ΛCDM cosmology and use it to compute the distances in each case, as in Fig. 10, together with the predicted AAP function from an N-body simulation of ΛCDM where α is measured directly from the simulation (green shaded region). It is clear that for $z < 1$ the INV model and the SUGRA model can be distinguished from the AAP function predicted in a ΛCDM cosmology. This result shows that if a SUGRA or INV model is the correct cosmology for the Universe, then ΛCDM can be ruled out. If there is a mismatch between the measurement from the observed pair sample and the simulation-calibrated AAP prediction as in Fig. 11, then a new simulation with a different expansion history is required until an acceptable match is found.
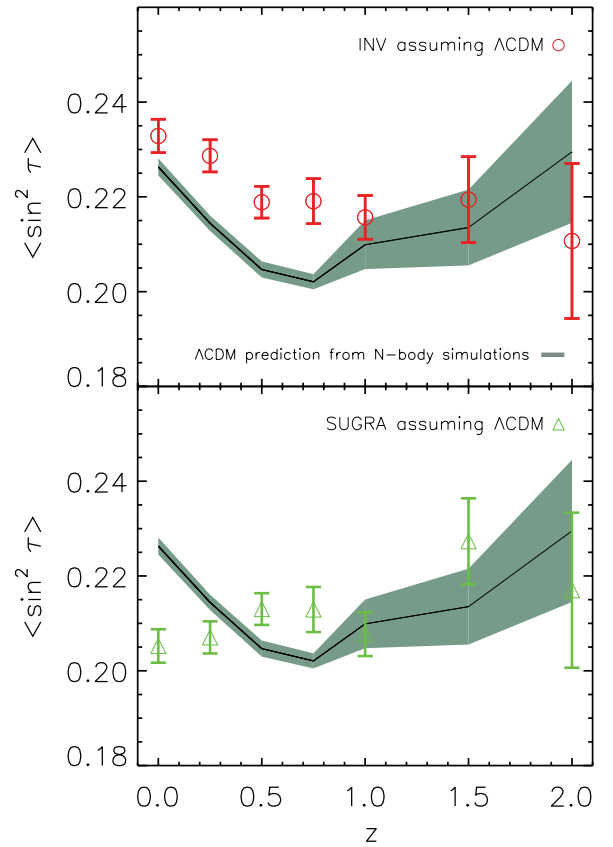
Figure 11. Upper panel: the measured mean of the anisotropic distribution of pairs of subhaloes in the INV dark energy simulation *assuming* a ΛCDM cosmology to find the comoving distance from each pair member (red circles). The predicted AAP function for a ΛCDM cosmology, using the value of α measured directly from the lower resolution N-body simulation, is shown as the solid black line. Lower panel: same as the upper panel but for the SUGRA quintessence model assuming a ΛCDM cosmology to determine comoving distances (green triangles).

6 SUMMARY

The distribution of the orientation of pairs of galaxies is uniform in real space in a homogeneous and isotropic universe. However, in redshift space, two effects lead to the inferred distribution becoming skewed. First, an observer has to assume a cosmology to convert positions on the sky and redshifts into distances. A mismatch between the assumed and underlying cosmologies introduces an error in the radial distance from a galaxy. Secondly, peculiar motions introduce distortions which break the connection between the measured redshift and the actual distance. Both effects result in an apparent displacement of galaxies along the line of sight.

Marinoni & Buzzi (2010) proposed that the distortion of the distribution of the angle subtended between galaxy pairs as viewed in redshift space can be modelled by a simple Doppler shift in the galaxy positions. This procedure gives rise to a theoretical prediction for the distribution in redshift space, which is referred to as the AAP function. We have tested the accuracy of this model using subhalo pairs identified in N-body simulations of cosmologies with different dark energy models.

The AAP function depends on two variables: the 'normalization' parameter $\alpha = H_0^{-1}(\langle\Delta v_\parallel^2/\Delta r^2\rangle)^{1/2}$ and the expansion history, $H(z)$, which depends on the cosmology. In this paper, we present the AAP function normalized in three different ways: (i) using the

relation $\alpha = H_0^{-1}(\langle\Delta v_{\parallel}^2/\Delta r^2\rangle)^{1/2}$, we can measure α directly from the simulation at each redshift; (ii) we can measure α at $z = 0$ by fitting to the measured distribution and then assume that α does not evolve with redshift, and apply the $z = 0$ normalization to specify the mean of the distribution of pairs at different redshifts (as suggested by Marinoni & Buzzi); and (iii) we can apply case (ii) but fitting for α at each redshift using the measured distribution and not just at $z = 0$. When we measure α directly (case i), we obtain excellent agreement between measurements of the mean from the simulation and the predictions of the AAP function. If instead we retain the best-fitting $z = 0$ value, $\alpha(z = 0)$, at each redshift (case ii), we do not find a good match between the theory and the simulation measurements. This demonstrates that simply fitting for α at $z = 0$ and assuming it does not evolve with redshift is not accurate. In fact such an approach would incorrectly rule out the cosmology used in the simulation. If we fit for α at each redshift using the simulation (case iii), then we again recover an excellent match between the theory and simulation results. We use a large sample of subhalo pairs which do not necessarily reside in fully relaxed and virialized haloes that have detached from the Hubble flow. This is demonstrated by the fact that we measure a different value for α in different cosmologies (see Section 5).

Note that each of the above cases considers idealized observers who know the correct cosmology to compute distances and $H(z)$. The measured mean of the distribution of pair angles (equation 1) depends on the cosmological model assumed to convert the position on the sky and redshift to comoving distance. The AAP function also depends on cosmology through $H(z)$. As a result, the measured mean and the AAP function will not agree if the wrong cosmology is assumed (the Alcock–Paczynski effect). Using two quintessence dark energy simulations (labelled INV and SUGRA), we have tested if the AAP function reproduces the measured mean of the distribution when, in the first instance, we know the correct cosmology (the 'perfect' observer case), and in the second instance, when we instead assume ΛCDM (i.e. the 'real' observer who has no prior knowledge of the underlying cosmology). The two dark energy models we consider have an evolving equation of state which is compatible with current observations of the cosmic microwave background, BAO and SN Ia distances. We find that, for a perfect observer who knows $H(z)$ and α exactly, the AAP function and the measured means are in very good agreement for both the SUGRA and the INV models.

Consider now performing the same exercise using the SUGRA and INV simulations, as a real observer who does not know the underlying cosmology and so assumes a ΛCDM cosmology, and who uses the best-fitting value for α at each redshift. We might expect that the theory should not match the measured mean for the dynamical dark energy models. However, we find that, by fitting for α using the observed distribution in the simulations, we instead recover a model which incorrectly matches the observations extremely well for both dark energy cosmologies, even though we have assumed a ΛCDM model. The consequences are that, in a universe with evolving dark energy, we would find that a ΛCDM model incorrectly matches the observations, invalidating the methodology.

In this paper, we have proposed a new formulation of the test of Marinoni & Buzzi in which the distribution of galaxy pairs can be analysed without prior knowledge of the cosmology. The measured distribution of angles should be compared with predictions for the AAP function using a reference N-body simulation to directly measure α. We have shown that the subhalo pairs in two quintessence dark energy simulations, which are treated as the 'observed' pair sample in this instance, produce a different measured distribution

from that predicted in a ΛCDM simulation even when analysed after assuming (incorrectly) a ΛCDM cosmology. In the new test, the AAP function is normalized with reference to a simulation with the same cosmology as assumed to analyse the observations. The predicted AAP function and measurement will only agree if the assumed cosmology matches the true cosmology. If this is not the case, then a new reference simulation must be generated with a revised expansion history, to see if an improved match to the observed distribution of galaxy pair angles can be obtained. We find that, by measuring the mean of the distribution as a function of redshift, we should be able to detect deviations from a ΛCDM expansion history at the level of 2 per cent in a box of volume $\sim 3\,h^{-3}\,\mathrm{Gpc}^3$. This new test complements the constraints on the present value of Hubble's parameter provided by observations of SNe Ia which constrain H_0 to ~ 3 per cent (Riess et al. 2011), and improves on constraints of $H(z)$ at higher redshifts which are accurate to about ~ 10 per cent.

7 CONCLUSIONS

Distinguishing between competing scenarios for the accelerating expansion of the universe is a major challenge for both observational and theoretical cosmologists. The expansion history and distance–redshift relations are remarkably close between viable models which satisfy the currently available constraints. A convincing determination of the nature of dark energy will require a combination of probes for two reasons (Albrecht et al. 2006). First, the small differences in the expected signals from a given probe mean that systematic effects become important. Applying different probes will allow us to see whether or not a measured signal is robust to systematics. Secondly, some existing tests cannot distinguish between some classes of dark energy model. New probes are therefore needed to break such degeneracies.

We have tested one such example of a new probe, the distribution of angles subtended between pairs of galaxies. This distribution is distorted by the peculiar motions of galaxies and also by the choice of cosmology adopted to transform observed positions into comoving distances. The origins of this test can arguably be traced back to Alcock & Paczynski (1979), and it was refined by Phillipps (1994). Marinoni & Buzzi (2010) applied the test to the angle between pairs of galaxies and crucially included redshift-space distortions.

We have used numerical simulations of structure formation to assess the performance of the test. The mean of the distribution of pair angles varies with redshift and, furthermore, is measurably different between cosmologies. A comparison between a theoretical model for the pair-angle distribution and the measurements from the simulations shows that the test, as originally proposed, is limited. The theoretical calculation requires a parameter to be specified to normalize the distribution of pair angles. Our simulations show that this parameter is redshift- and cosmology-dependent.

It is possible to estimate the normalization of the pair-angle distribution observationally, at redshifts $z > 0$, if the peculiar velocities of galaxies can be measured. For example, it was recently argued that accurate mean pairwise velocities of pairs of SNe Ia can be obtained by combining photometry from a survey such as the Pan-STARRS (Kaiser et al. 2010) or the Large Synoptic Survey Telescope (Abell et al. 2009) with follow-up spectroscopy (Bhattacharya et al. 2011). At present, the accuracy of measurements of the peculiar velocity field is not adequate to distinguish between the models compared in this paper.

Our proposed methodology avoids this problem by using an N-body simulation with a similar number of pairs to the observational sample to normalize the distribution of angles. This secures the

crucial step of setting the normalization of the theoretical distribution at each redshift. The detailed selection of the *N*-body sample of subhalo pairs is not important, avoiding the need to combine the simulation with a galaxy formation model. Furthermore, we have demonstrated that it is not necessary to have a knowledge of the true underlying background cosmology for the successful application of the test.

The new method we have proposed is a powerful complement and extension to existing probes of dark energy. This is demonstrated by the ability of the pair distribution to distinguish between cosmologies that cannot be separated through the appearance of BAOs or through the halo mass function. The technique can be applied already to ongoing surveys, such the SDSS-III BOSS (Schlegel et al. 2007), and should yield competitive constraints. The method should also produce distinct signals for dark energy and modified gravity models which have identical expansion histories, through the different peculiar motions induced.

REFERENCES

Abazajian K. N. et al., 2009, ApJS, 182, 543
Abell P. A. et al. (LSST Science Collaborations), 2009, preprint (arXiv:0912.0201)
Albrecht A. et al., 2006, preprint (arXiv:astro-ph/0609591)
Alcock C., Paczynski B., 1979, Nat, 281, 358
Almeida C., Baugh C. M., Wake D. A., Lacey C. G., Benson A. J., Bower R. G., Pimbblet K., 2008, MNRAS, 386, 2145
Angulo R., Baugh C. M., Frenk C. S., Lacey C. G., 2008, MNRAS, 383, 755
Baugh C. M., Gaztanaga E., Efstathiou G., 1995, MNRAS, 274, 1049
Bernardi M. et al., 2001, preprint (arxiv:astro-ph/0110344)
Bhattacharya S., Kosowsky A., Newman J. A., Zentner A. R., 2011, Phys. Rev. D, 83, 043004
Blake C. et al., 2010, MNRAS, 406, 776
Blake C. et al., 2011, doi:10.1111/j.1365-2966.2011.19606
Blakeslee J. P., Davis M., Tonry J. L., Ajhar E. A., Dressler A., 2000, in Courteau S., Strauss M. A., Willick J. A., eds, ASP Conf. Ser. Vol. 201, Cosmic Flows 1999: Towards an Understanding of Large-Scale Structure. Astron. Soc. Pac., San Francisco, p. 352
Borgani S., da Costa L. N., Zehavi I., Giovanelli R., Haynes M. P., Freudling W., Wegner G., Salzer J. J., 2000, AJ, 119, 102
Brax P., Martin J., 1999, Phys. Lett. B, 468, 40
Coil A. L. et al., 2004, ApJ, 609, 525
Copeland E. J., Sami M., Tsujikawa S., 2006, Int. J. Mod. Phys. D, 15, 1753
Corasaniti P. S., Copeland E. J., 2003, Phys. Rev. D, 67, 063521

Courteau S., Willick J. A., Strauss M. A., Schlegel D., Postman M., 2000, ApJ, 544, 636
da Costa L. N. et al., 2000, AJ, 120, 95
Davis M., Efstathiou G., Frenk C. S., White S. D. M., 1985, ApJ, 292, 371
Fang W., Hu W., Lewis A., 2008, Phys. Rev. D, 78, 087303
Ferreira P. G., Joyce M., 1998, Phys. Rev. D, 58, 023503
Guzzo L. et al., 2008, Nat, 451, 541
Hamilton A. J. S., 1998, Ap&SS, 231, 185
Jennings E., Baugh C. M., Angulo R. E., Pascoli S., 2010, MNRAS, 401, 2181
Jennings E., Baugh C. M., Pascoli S., 2011a, MNRAS, 410, 2081
Jennings E., Baugh C. M., Pascoli S., 2011b, ApJ, 727, L9
Kaiser N. et al., 2010, Proc. SPIE Vol. 7733. SPIE, Bellingham, p. 12
Komatsu E. et al., 2010, ApJS, 192, 18
Kowalski M. et al., 2008, ApJ, 686, 749
Laureijs R. J., Duvet L., Escudero Sanz I., Gondoin P., Lumb D. H., Oosterbroek T., Saavedra Criado G., 2010, in Oschmann J. M., Jr, Clampin M. C., MacEwen H. A., eds, Proc. SPIE Vol. 7731, Space Telescopes and Instrumentation 2010: Optical, Infrared, and Millimeter Wave. SPIE, Bellingham
Lewis A., Bridle S., 2002, Phys. Rev. D, 66, 103511
Marinoni C., Buzzi A., 2010, Nat, 468, 539
Martin J., 2008, Mod. Phys. Lett. A, 23, 1252
Massey R. et al., 2007, Nat, 445, 286
Montesano F., Sánchez A. G., Phleps S., 2010, MNRAS, 408, 2397
Montesano F., Sanchez A. G., Phleps S., 2011, preprint (arXiv:1107.4097)
Norberg P., Baugh C. M., Gaztañaga E., Croton D. J., 2009, MNRAS, 396, 19
Nusser A., Branchini E., Davis M., 2011, preprint (arXiv:1106.6145)
Okumura T., Jing Y. P., 2011, ApJ, 726, 5
Peacock J. A., Schneider P., Efstathiou G., Ellis J. R., Leibundgut B., Lilly S. J., Mellier Y., 2006, Technical Report by the ESA-ESO Working Group on 'Fundamental Cosmology'. Available at http://arxiv.org/abs/astro-ph/0610906
Percival W. J. et al., 2007, MNRAS, 381, 1053
Perlmutter S. et al., 1999, ApJ, 517, 565
Phillipps S., 1994, MNRAS, 269, 1077
Ratra B., Peebles P. J. E., 1988, Phys. Rev. D, 37, 3406
Riess A. G. et al., 1998, ApJ, 116, 1009
Riess A. G. et al., 2011, ApJ, 730, 119
Sánchez A. G., Baugh C. M., Angulo R., 2008, MNRAS, 390, 1470
Sánchez A. G., Crocce M., Cabré A., Baugh C. M., Gaztañaga E., 2009, MNRAS, 400, 1643
Schlegel D. J. et al., 2007, BAAS, 38, 132.29
Schlegel D. J. et al., 2009, Am. Astron. Soc. Meeting Abs, preprint (arXiv:0904.0468)
Schlegel D. et al., 2011, Am. Astron. Soc. Meeting Abs, preprint (arxiv e-prints)
Seo H.-J., Eisenstein D. J., 2007, ApJ, 665, 14
Seo H.-J., Siegel E. R., Eisenstein D. J., White M., 2008, ApJ, 686, 13
Smith R. E. et al., 2003, MNRAS, 341, 1311
Smith R. E., Scoccimarro R., Sheth R. K., 2007, Phys. Rev. D, 75, 063512
Smith R. E., Scoccimarro R., Sheth R. K., 2008, Phys. Rev. D, 77, 043525
Springel V., 2005, MNRAS, 364, 1105
Springel V., White S. D. M., Tormen G., Kauffmann G., 2001, MNRAS, 328, 726
Tonry J. L. et al., 2001, ApJ, 546, 681
Wang Y., 2008, J. Cosmol. Astropart. Phys., 0805, 021
White S. D. M., 1994, Rev. Mod. Astron., 7, 255
White M. et al., 2011, ApJ, 728, 126
Zlatev I., Wang L.-M., Steinhardt P. J., 1999, Phys. Rev. Lett., 82, 896

This paper has been typeset from a TEX/LATEX file prepared by the author.